

Imaging Enhancement Through Deep Learning Aided Decompression in Ultrasound Tomography

Abstract. The research aimed to develop a method that could automatically decompress and filter images of transmission ultrasound tomography. The novelty of the presented method is an algorithm that automates improving the quality of tomograms through deep learning. Another innovation is using the original method of automatic filtering of tomographic images.

Streszczenie. Celem badań było opracowanie metody umożliwiającej automatyczną dekompresję i filtrację obrazów w transmisyjnej tomografii ultradźwiękowej. Nowością prezentowanej metody jest algorytm automatyzujący proces poprawy jakości tomogramów poprzez zastosowanie głębokiego uczenia. Kolejną innowacją jest wykorzystanie autorskiej metody automatycznego filtrowania obrazów tomograficznych (Poprawa obrazowania za pomocą dekompresji wspomaganej głębokim uczeniem w tomografii ultradźwiękowej).

Keywords: ultrasound tomography; image compression; discrete cosine transform; machine learning.

Słowa kluczowe: tomografia ultradźwiękowa; kompresja obrazu, dyskretna transformata kosinusowa, uczenie maszynowe.

Introduction

Ultrasound tomography (UST) is a non-invasive imaging technique that utilizes ultrasonic waves to visualise the subject's internal structure under investigation. This process involves the emission of sound waves by ultrasonic sensors, traverse the object and are received by the same or different sensors. Depending on the specific type of tomography, the sensors may gather information about the time of flight of the sound wave through the object or its amplitude. These data are subsequently processed by a complex electronic system that reconstructs an image of the interior of the examined object. This process can be mathematically intricate, especially when the number of measurements is limited relative to the number of pixels in the reconstructed image [1-8]. Ultrasound tomography finds application in various fields. In medicine, it is employed for imaging different body parts such as the heart, liver, kidneys, and reproductive system, allowing for the diagnosis and monitoring of various health conditions. In engineering and materials research, this technique can be used to analyse the structure and properties of various materials, including detecting defects and cracks. In geology, ultrasonic tomography can provide valuable insights into the structure of rocks and soils, bearing significance in seismic and environmental studies. This technique is often used in industry for quality control, such as assessing welds and other structural connections [9-15].

The Discrete Cosine Transform (DCT) is a mathematical function that plays a pivotal role in digital signal processing. It transforms a signal or image from the spatial or temporal domain into the frequency domain, representing the signal as a sum of cosine functions oscillating at varying frequencies. This transformation is achieved through mathematical operations that convert the original data into a set of frequency components, each corresponding to a specific cosine wave. One of the key attributes of DCT is its ability to concentrate the signal energy into a few significant frequency components. This characteristic is particularly valuable in signal processing and data compression applications, where it enables the representation of the essential features of the data with fewer coefficients. By focusing on the most important frequency components, DCT reduces data size without substantially losing quality. In the realm of image and video compression, DCT's efficiency has led to its incorporation into widely adopted standards such as JPEG for image and MPEG for video compression. In these applications, DCT works by dividing

the image or video frame into smaller blocks and then applying the transformation to each block. The resulting frequency components are then quantized and encoded, leading to a compressed representation of the original data. This process facilitates efficient storage and transmission and provides a mechanism for controlling the trade-off between compression ratio and quality.

Furthermore, DCT has applications beyond compression. It is used in various filtering techniques, noise reduction, and pattern recognition tasks. Its ability to represent data in the frequency domain provides insights into the underlying patterns and characteristics of the signal, making it a versatile tool in analytical and diagnostic applications.

In our previous works, we have explored and described the mathematical foundations of this method, its implementation details, and its applications in various domains. [16-18]

Due to the high level of compression, there is a problem with removing artifacts in the Blockwise Transform Reduction, even though it is a fast and efficient reconstruction method [18, 20]. In the original method, static Gaussian filtering and global thresholding were implemented. That kind of filtering has proven to be sufficient but requires manual parameter selections. Furthermore, the availability of suitable learning data sets, i.e., matrices of real measurement data paired with the corresponding ground-truth images, limits the application of machine learning in the topic. The research aims to develop a method for a compressed form of reconstructions that can automatically decompress and filter images of transmission ultrasound tomography (UST). The novelty of the presented method is an algorithm that automates the process of improving the quality of UST tomograms through deep learning with minimal demand for basic tomographic images. Another innovation is using the original method of automatic filtering of tomographic images.

Materials and Methods

The primary area of application of UST is medicine. UST is used to examine the internal organs of the human body, such as the breast or bladder. The accuracy of imaging is critical because human health and life depend on it. The main thing that makes it hard to get high-quality tomograms is having to solve the inverse problem that comes with turning the measurement vector into images. The difficulty of the inverse problem is due to insufficient input

information, which results in imprecise output values. In these studies, the tomographic image is created on a grid of squares with a resolution of 64×64, which means that the model creating the tomographic images must generate 2304 output values. These are real numbers that are converted to colors. This way, an image is created on a matrix with a resolution of 64×64. This concept's originality is reducing the input information deficit effect by compressing the output image. In this case, the neural network's architecture is ignored because the method discussed here relates to the way CNN is used, not its structure. Discrete Cosine Transform (DCT) was used as the compression method [18]. Let's assume that $A(m,n)$ is the m,n^{th} element of the original, uncompressed image represented by the matrix A . The DCT basis images F_{pq}^{DCT} are described by the formula (1), which determines one entry p,q^{th} of the DCT transformed matrix calculated from the pixel values of the uncompressed image A .

$$(1) \quad F_{pq}^{DCT} = \alpha_p \alpha_q \cos \frac{\pi(2m+1)p}{2M} \cos \frac{\pi(2n+1)q}{2N}$$

where N, M are the sizes of the block that the DCT is done, and

$$\alpha_p = \begin{cases} 1/\sqrt{M} & p = 0 \\ \sqrt{2/M} & 1 \leq p \leq M - 1 \end{cases}, \alpha_q = \begin{cases} 1/\sqrt{M} & q = 0 \\ \sqrt{2/M} & 1 \leq q \leq M - 1 \end{cases}$$

For the original, uncompressed image matrix A_{mn} the matrix of coefficients in the DCT base is described by (2).

$$(2) \quad B_{pq} = \alpha_p \alpha_q \sum_{m=0}^{M-1} \sum_{n=0}^{N-1} A_{mn} \cos \frac{\pi(2m+1)p}{2M} \cos \frac{\pi(2n+1)q}{2N}$$

Reconstructed compression b_{rec} can be obtained from the measurement vector m with a formula (3)

$$(3) \quad b_{rec} = (J_{DCT}^T J_{DCT} + \lambda I)^{-1} J_{DCT}^T m$$

where J_{DCT} is a compressed form of a sensitive matrix, and λ is a numerical error regularization parameter.

Figure 1 shows the view of the test stand used to validate the described concept. On the left-hand side, there is a tank filled with tap water. The edge of the tank was made of plexiglass with a thickness of 3 millimetres. A plastic tube acts as an inclusion in the middle of the tank. There are UST transducers around the reservoir. The transducers used were in positions opposite each other at a distance of 20 cm. It can see the tomograph prototype on the right side, completely designed and made in our Research and Development Centre, Netrix laboratory.



Fig.1. Physical model for validation of image reconstructions based on UST measurements.

Figure 2 shows the operating principle of the described concept. In the first step, we train a standard model, CNN_1 , to turn the measurement vector X into compressed tomographic images B_1 .

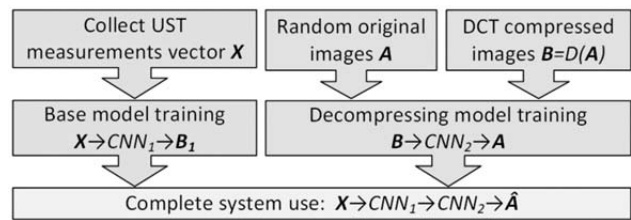


Fig.2. The UST system works, using imaging enhancement with deep learning-aided decompression.

The second step is to train the convolutional neural network (CNN_2) to decompress the images. The pattern image in the form of the DCT coefficient matrix B is the input for the CNN_2 . At the CNN_2 output are decompressed reconstructions of the pattern image A . It is easy to see that to train this kind of CNN_2 model, no real observations in the form of matrices of real measurement data paired with the corresponding ground-truth images are needed. This is a very important benefit because one of the biggest problems with machine learning is that it needs many observations to train. The entire process of UST image reconstruction \hat{A} with the use of a CNN_2 decompressor can be written in the form of $X \rightarrow CNN_1 \rightarrow CNN_2 \rightarrow \hat{A}$. Figure 3 shows the way of using the convolutional neural network as a system that transforms compressed DCT images B_1 into output images \hat{A} .

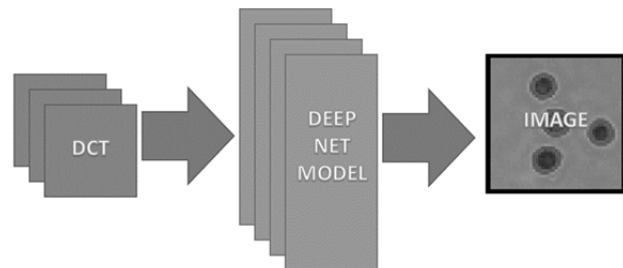


Fig.3. The concept of using CNN as a DCT decompressor.

The DCT function is deterministic, so any image is decompressed similarly, no matter what it shows. The quality loss caused by DCT compression is correlated with the pixel values of the uncompressed original image matrix. Therefore, it can generate reference images for the training set by creating images containing random inclusion distributions. The training set is given the matrices of DCT coefficients that go with these images.

Testing of Integrated Elements of the Measurement System

In order to test the integrated measurement card, which is connected to two ultrasonic transducers with a frequency of 40kHz, test measurements were made to check the correct operation of the system and to assess the levels of measurement noise (Figure 4).

The measurement data were sent to a PC via a USB port, where they were analyzed. To increase the repeatability of measurements, transducers from a tomographic probe were used; this eliminated the problem of stabilizing the mutual position of the transducers and allowed for testing in conditions close to real ones.

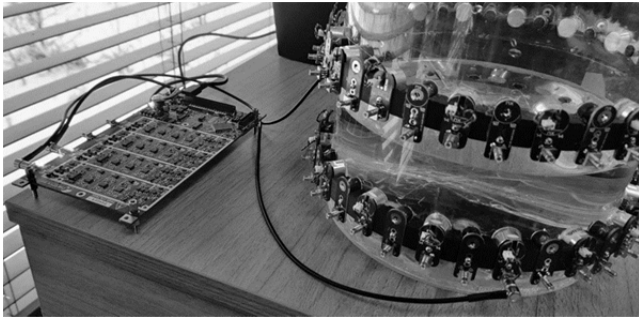


Fig.4. View of the measurement card and measurement station.

As an integrated measurement card, the tested element worked properly and showed no programming errors related to the measurement and data transfer. Using a multiplier in the second amplification stage increased the maximum standard deviation of the measured values (Figure 5).

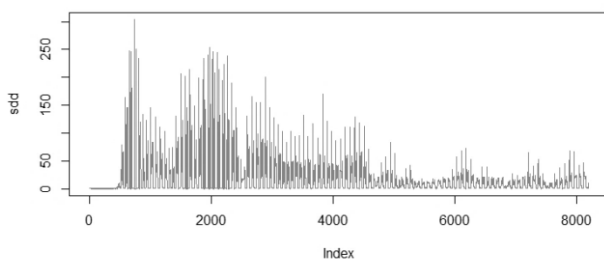


Fig.5. Standard deviation of measurements (Number of transmitter pulses: 3, Level I gain: 20dB, Level II gain 2 V/V Sample frequency: 3MHz, Number of samples: 8192, Number of repetitions: 100).

In the case of a 20 cm measuring probe, a multiplier of 1/1 V/V was sufficient (Figure 6).

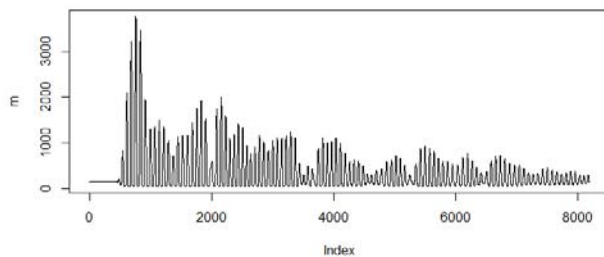


Fig.6. Average measurements. Reduction of the second gain threshold to 1-fold (Transmitter pulse count: 3, First-level gain: 20dB, Second-level gain: 1 V/V, Sampling frequency: 3MHz, Number of samples: 8192, Number of repetitions: 100).

The introduction of envelope filtering significantly reduced the range of the coefficient of variation. The skewness coefficient varied symmetrically in the range of less than +/- 1. (Figure 7)

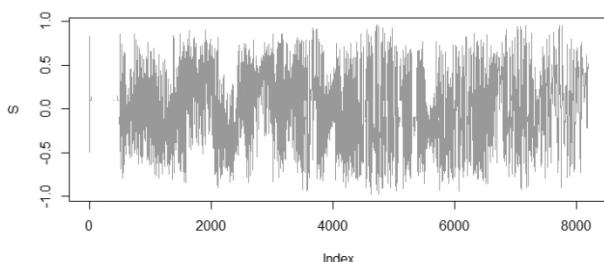


Fig.7. Coefficient of skewness. (Envelope Measurements: Number of transmitter pulses: 3, Level I gain: 20dB, Level II gain 1 V/V Sample frequency: 3MHz, Number of samples: 8192, Number of repetitions: 100).

Selected tests suggested non-normal dispersion of measurements of single samples, but in most cases, they were unimodal; the histograms of the measurements were also unimodal (Figure 8).

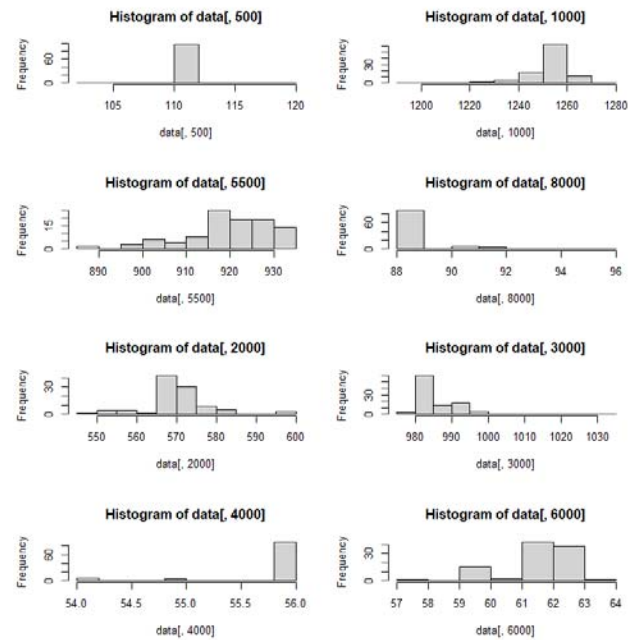


Fig.8. Histograms of selected samples.

Results and Conclusions

Figure 9 compares the results obtained using the CNN2 decompressor with reference images. Two cases are for single inclusions, and the others are for four. The reconstruction images reflect the model images with high fidelity. A high similarity level relates to the inclusions' position, size, and shape hidden inside the tested tank.

Cases with a single inclusion		Cases with many inclusions	
Pattern A	Output \hat{A}	Pattern A	Output \hat{A}

Fig.9. Comparison of the results obtained by the CNN₂ decompressor with reference images.

The results indicate that the solution presented in this study, consisting of reducing the dependent (output) variables by image compression using the DCT method and their decompression using a convolutional neural network, is effective and efficient. The two-step approach achieves better results than the conventional method without image compression and decompression. It is also important that the described concept be effective for various machine learning models. While we verified CNN in these studies, it is quite logical and reasonable that other methods will also be useful. So, it is a reliable and universal approach.

Authors: Konrad Kania, M.Sc. Eng., Lublin University of Technology, Nadbystrzycka 38A, Lublin, Poland E-mail: k.kania@pollub.pl; Grzegorz Kłosowski, Ph.D., Lublin University of Technology, Nadbystrzycka 38A, Lublin, Poland, E-mail: g.klosowski@pollub.pl; Mariusz Mazurek, Ph.D., Institute of Philosophy and Sociology of the Polish Academy of Science Warsaw, Poland, E-mail: mmazurek@ifispan.edu.pl; Józef Stokłosa, Ph.D., D.Sc. Eng., WSEI University, Projektowa 4, Lublin, Poland E-mail: jozef.stoklosa@wsei.lublin.pl.

REFERENCES

- [1] Herman, G.T. Image Reconstruction from Projections: The Fundamentals of Computerised Tomography, Academic Press, New York, (1980).
- [2] Beck, M. S.; Williams, R. A. Process tomography: A European innovation and its applications. *Meas. Sci. Technol.* 7 (1996), No. 3, 215–224.
- [3] Kak, AC; Slaney, M. Principles of Computerized Tomographic Imaging, IEEE Press, New York, 1999.
- [4] Kłosowski G., Rymarczyk T., Niderla K., Kulisz M., Skowron Ł., Soleimani M., Using an LSTM network to monitor industrial reactors using electrical capacitance and impedance tomography – a hybrid approach. *Eksploracja i Niezawodność – Maintenance and Reliability*, 25 (2023), No. 1, 11.
- [5] Kłosowski G., Rymarczyk T., Kania K., Świć A., Cieplak T., Maintenance of industrial reactors supported by deep learning driven ultrasound tomography, *Eksploracja i Niezawodność – Maintenance and Reliability*; 22 (2020), No 1, 138–147.
- [6] Kłosowski G., Rymarczyk T., Niderla K., Rzemieniak M., Dmowski A., Maj M., Comparison of Machine Learning Methods for Image Reconstruction Using the LSTM Classifier in Industrial Electrical Tomography, *Energies* 2021, 14 (2021), No. 21, 7269.
- [7] Rymarczyk T., Kłosowski G., Hoła A., Sikora J., Tchórzewski P., Skowron Ł., Optimising the Use of Machine Learning Algorithms in Electrical Tomography of Building Walls: Pixel Oriented Ensemble Approach, *Measurement*, 188 (2022), 110581.
- [8] Koulountzios P., Rymarczyk T., Soleimani M., A triple-modality ultrasound computed tomography based on full-waveform data for industrial processes, *IEEE Sensors Journal*, 21 (2021), No. 18, 20896–20909.
- [9] Soetomo, K.; Rahma, TF; Juliastuti, E.; Kurniadi, D. Ultrasonic tomography for reinforced concrete inspection using algebraic reconstruction technique with Iterative Kaczmarz method. In Proceedings of the 2016 International Conference on Instrumentation, Control and Automation (ICA), Bandung, Indonesia, 29–31 August 2016; IEEE: Piscataway, NJ, USA, (2016); 16–21.
- [10] Yan, B.; Wu, C.; Ma, H. Study on the method of nonmetallic defects based on ultrasonic tomography and morphology. In Proceedings of the 2017 12th IEEE Conference on Industrial Electronics and Applications (ICIEA), Siem Reap, Cambodia, 18–20 June 2017; IEEE: Piscataway, NJ, USA, (2017); 1287–1292.
- [11] Rahman Mohd Yunus, F.; Azida Noor Azlan, N.; Nor Ayob, N.M.; Pusppanathan, J.; Fahajumi Jumaah, M.; Chiew Loon, G.; Abdul Rahim, R.; Ahmad, A.; Md Yunus, Y.; Rahim, H. Simulation Study of Bubble Detection Using Dual-Mode Electrical Resistance and Ultrasonic Transmission Tomography for Two-Phase Liquid and Gas. *Sens. Transducers*, 150 (2013), 97–105.
- [12] Koulountzios P., Aghajanian S., Rymarczyk T., Koiranen T., Soleimani M., An Ultrasound Tomography Method for Monitoring CO2 Capture Process Involving Stirring and CaCO3 Precipitation, *Sensors*, 21 (2021), No. 21, 6995.
- [13] Gnaś, D., Adamkiewicz, P., Indoor localization system using UWB, *Informatyka, Automatyka, Pomiary W Gospodarce I Ochronie Środowiska*, 12 (2022), No. 1, 15-19.
- [14] Goćławski, J., Sekulska-Nalewajko, J., Korzeniewska, E., Prediction of textile pilling resistance using optical coherence tomography, *Scientific Reports*, 12 (2022), No. 1, 18341.
- [15] Goćławski, J., Korzeniewska, E., Sekulska-Nalewajko, J., Kiełbasa, P., Drózdź, T., Method of Biomass Discrimination for Fast Assessment of Calorific Value, *Energies*, 15 (2022), No. 7, 2514.
- [16] Mazurek, M., Rymarczyk, T., Kania, K., & Kłosowski, G. Dedicated algorithm based on discrete cosine transform for the analysis of industrial processes using ultrasound tomography. *Adjunct Proceedings of the 2020 ACM International Joint Conference on Pervasive and Ubiquitous Computing and Proceedings of the 2020 ACM International Symposium on Wearable Computers*, (2020).
- [17] Mazurek, M., Rymarczyk, T., Kłosowski, G., Maj, M., & Adamkiewicz, P. Tomographic measuring sensors system for analysis and visualization of technological processes. *2020 50th Annual IEEE-IFIP International Conference on Dependable Systems and Networks-Supplemental Volume (DSN-S)*, (2020).
- [18] Styła, M., Adamkiewicz, P., Optimisation of commercial building management processes using user behaviour analysis systems supported by computational intelligence and RTI, *Informatyka, Automatyka, Pomiary W Gospodarce I Ochronie Środowiska*, 12 (2022), No 1, 28-35.